

The dynamics of Alzheimer's disease biomarkers in the Alzheimer's Disease Neuroimaging Initiative cohort

A. Caroli^{a,b,*}, G.B. Frisoni^a, The Alzheimer's Disease Neuroimaging Initiative[†]

^a LENITEM Laboratory of Epidemiology, Neuroimaging and Telemedicine, IRCCS S. Giovanni di Dio-FBF, Brescia, Italy

^b Medical Imaging Unit, Biomedical Engineering Department, Mario Negri Institute for Pharmacological Research, Bergamo, Italy

Received 14 February, 2010; received in revised form 21 April 2010; accepted 22 April 2010

Abstract

The aim of this study was to investigate the dynamics of four of the most validated biomarkers for Alzheimer's disease (AD), cerebro-spinal fluid (CSF) $A\beta$ 1–42, tau, hippocampal volume, and FDG-PET, in patients at different stage of AD. Two hundred twenty-nine cognitively healthy subjects, 154 mild cognitive impairment (MCI) patients converted to AD, and 193 (95 early and 98 late) AD patients were selected from the Alzheimer's Disease Neuroimaging Initiative (ADNI) database. For each biomarker, individual values were Z-transformed and plotted against ADAS-cog scores, and sigmoid and linear fits were compared. For most biomarkers the sigmoid model fitted data significantly better than the linear model. $A\beta$ 1–42 time course followed a steep curve, stabilizing early in the disease course. CSF tau and hippocampal volume changed later showing similar monotonous trends, reflecting disease progression. Hippocampal loss trend was steeper and occurred earlier in time in APOE ϵ 4 carriers than in non-carriers. FDG-PET started changing early in time and likely followed a linear decline. In conclusion, this study provides the first evidence in favor of the dynamic biomarker model which has recently been proposed.

© 2010 Elsevier Inc. All rights reserved.

Keywords: Alzheimer's disease; Alzheimer's Disease Neuroimaging Initiative dataset; Biomarker dynamics; Cerebro-spinal fluid $A\beta$ 42; Tau; Hippocampal volume; FDG-PET

Most of the Alzheimer disease (AD) research between the years 2000 and 2010 has been focused on finding biomarkers which could be reliably used to diagnose AD, monitor its progression, and predict its onset. A number of fluid and imaging biomarkers have been identified and validated (Hampel et al., 2008; Shaw et al., 2007), the most studied to date being $A\beta$ plaque deposition (assessed either in terms of reductions in cerebro-spinal fluid (CSF) $A\beta$

1–42 or increased amyloid positron emission tomography (PET) tracer retention), CSF tau, fluoro-deoxy-glucose (FDG) uptake on PET, and structural magnetic resonance imaging (MRI).

Evidence from several past studies strongly supports the notion that amyloid Pittsburgh Compound B (PIB)-PET (Klunk et al., 2004; Rowe et al., 2007; Edison et al., 2007, Ikonomic et al, 2008) and low CSF $A\beta$ 1–42 (Clark et al., 2003; Fagan et al., 2006; Schoonenboom et al., 2008; Strozyk et al., 2003; Tapiola et al., 2009) are valid biomarkers for brain $A\beta$ plaque load. Increased CSF tau, despite being not specific to AD, is an indicator of tau pathological changes and neuronal injury, and correlates with clinical disease severity (Arai et al., 1995; Blennow et al., 1995; Buerger et al., 2006; Hansson et al., 2006; Shaw et al., 2009; Tapiola et al., 2009). FDG-PET measures brain metabolism and is a valid indicator of the synaptic dysfunction that accompanies neurodegeneration in AD (Hoffman et al.,

* Corresponding author at: Laboratory of Epidemiology, Neuroimaging and Telemedicine IRCCS San and Giovanni di Dio-FBF. Via Pilastroni 4, 25125, Brescia, Italy. Tel: +39 030 3501361; fax: +39 02 700435727.

E-mail address: acaroli@fatebenefratelli.it (A. Caroli).

[†] Data used in the preparation of this article were obtained from the ADNI database (www.loni.ucla.edu/ADNI). As such, the investigators within the ADNI contributed to the design and implementation of ADNI and/or provided data but did not participate in analysis or writing of this report. A complete listing of ADNI investigators is available at: www.loni.ucla.edu/ADNI/Collaboration/ADNI_Authorship_list.pdf.

2000; Jagust et al., 2007; Minoshima et al., 1997). Structural MRI measures cerebral atrophy, which is not specific to AD but strictly correlates with the disease severity even at latest stages, and can be considered a valid biomarker of neurodegeneration (Bobinski et al., 2000; Frisoni et al., 2010; Gosche et al., 2002; Silbert et al., 2003; Zarow et al., 2005); among all MRI-based markers, hippocampal volume has been widely shown to be one of the most reliable (Jack et al., 2000; Schuff et al., 2009; Van de Pol et al., 2006).

Biomarkers have allowed to further understand the pathology underlying AD, pointing out that a dichotomous view (people with AD pathology have dementia, people without AD pathology have not), common in the past, cannot hold any more, and should be replaced by a more dynamic picture, in which pathologic and clinical changes occur gradually over time. Several studies have shown that biomarker abnormalities precede clinical symptoms. Autopsy brain studies found no strict relationship between quantitative measures of cortical amyloid deposition and the duration and severity of Alzheimer disease (Ingelsson et al., 2004). Jack and colleagues showed that many of normal controls are PIB positive, suggesting that plaque deposition occurs before neurodegeneration (Jack et al., 2008a), and showed that PIB retention (i.e. amyloid load) increase occurs in prodromal AD, being almost stable in time in the clinical phases of the disease (Jack et al., 2009).

The availability of several validated biomarkers opens the discussion about how to choose among them: which marker is better to use to diagnose AD? Which better predicts AD? All these markers are validated enough to be used in active therapeutic trials or large longitudinal observational studies, but which is better to use to track cognitive decline or monitor new drugs therapeutical efficacy?

Jack and colleagues (Jack et al., 2010) pointed out that individual biomarkers, reflecting individual aspects of the Alzheimer pathology, develop on their own time course, and do not become abnormal or steady simultaneously.

The open challenge, now, is to try to order biomarker changes in time. This would enable us to express the disease process in terms of a series of testable biological indicators, and thus to identify biomarkers which could be best used in clinical trials to select patients and measure disease-modifying drug effects, or even be used in future prevention trials. Furthermore, understanding the temporal order of each biomarker would make it possible to use a given marker for staging AD *in vivo*.

Among the most validated biomarkers described above, A β 1–42 deposition was reported to change first, as early as 20 years before symptoms appear, but quickly reach a plateau by the time a person has dementia (Jack et al., 2008a; Jack et al., 2009). Structural changes become appreciable later in the disease process, but correlate with cognitive progression as dementia worsens (Jack et al., 2008a; Jack et al., 2009; Vemuri et al., 2009). The synaptic dysfunction marker FDG-PET and the neurodegeneration marker CSF

tau are supposed to lie between A β 1–42 and MRI (Jack et al., 2010; Reiman et al., 1998), but there is lack of evidence about it. Furthermore, long-term biomarker dynamics has been hypothesized to be nonlinear, likely sigmoid shape (Jack et al., 2010).

The aim of this study is to use the Alzheimer's Disease Neuroimaging Initiative (ADNI) dataset to investigate the dynamics of four of the most validated AD biomarkers (CSF A β 1–42, CSF tau, hippocampal volume, and FDG uptake on PET) in a cohort of cognitively healthy subjects and AD patients at different stage of disease.

1. Methods

1.1. Subjects

Data used in the preparation of the current paper were obtained from the ADNI database (www.loni.ucla.edu/ADNI). The ADNI was launched in 2003 by the National Institute on Aging (NIA), the National Institute of Biomedical Imaging and Bioengineering (NIBIB), the Food and Drug Administration (FDA), private pharmaceutical companies, and nonprofit organizations, as a US \$60 million, 5 year public-private partnership. The ADNI primary goal has been to test whether serial MRI, PET, other biological markers, and clinical and neuropsychological assessment can be combined to measure the progression of mild cognitive impairment (MCI) and early AD. Determination of sensitive and specific markers of very early AD progression is intended to aid researchers and clinicians to develop new treatments and monitor their effectiveness, as well as lessen the time and cost of clinical trials. The Principle Investigator of this initiative is Michael W. Weiner MD, VA Medical Center and University of California, San Francisco. ADNI is the result of efforts of many coinvestigators from a broad range of academic institutions and private corporations, and subjects have been recruited from over 50 sites across the USA and Canada. The initial goal of ADNI was to recruit 800 adults, ages 55 to 90, to participate in the research – approximately 200 cognitively normal older individuals to be followed for 3 years, 400 people with MCI to be followed for 3 years, and 200 people with early AD to be followed for 2 years. For up-to-date information see www.adni-info.org.

At baseline, all subjects were given the American National Adult Reading Test and the following cognitive measures were examined: digit span, category fluency, Trail Making A and B, Digit Symbol Substitution Test of the Wechsler Adult Intelligence Scale–Revised, Boston Naming Test, Auditory Verbal Learning Test, clock drawing, Neuropsychiatric Inventory Q, AD Assessment Scale–Cognitive Subscale, and Functional Assessment Questionnaire (Cummings et al., 2005; Kaplan et al., 1982; Reitan, 1958; Rey, 1964; Rosen et al., 1984; Wechsler, 1987); they underwent blood drawing (for APOE genotyping) and struc-

tural MR. Subsets of subjects underwent lumbar puncture (for CSF sampling), FDG-PET or PIB-PET.

Healthy controls (HC) were all those in the ADNI database with available ADAS-Cog score ($n = 229$). We then considered ADNI patients with baseline diagnosis of MCI who had progressed to AD during the ADNI project observation time ($n = 154$, conversion time 6 to 36 months). We finally considered all ADNI AD patients, and we divided them in two groups of similar size according to the Mini Mental State Examination (MMSE) score: early AD, with MMSE score above the 50th percentile ($MMSE > 23$, $n = 95$), and late AD, with MMSE score below the 50th percentile ($MMSE \leq 23$, $n = 98$).

1.2. Cerebro-spinal fluid measurements

Methods for CSF acquisition and biomarker measurement used in the ADNI study have been reported previously (Shaw et al., 2009). In brief, CSF was collected, transferred to polypropylene tubes, and frozen on dry ice within an hour after collection. Samples were divided into aliquots at the University of Pennsylvania ADNI Biomarker Core Laboratory, stored at -80°C , and measured using the multiplex xMAP Luminex platform (Luminex, Corp, Austin, TX) with Innogenetics (INNOBIA AlzBio3, Ghent, Belgium) immunoassay kit-based reagents as previously described (Olsson et al., 2005). The reagents included monoclonal antibodies specific for $A\beta$ 1–42 (4D7A3), t-tau (AT120) and p-tau phosphorylated at threonine 181 (AT270), and analyte-specific detector antibodies (HT7, 3D6). In the current study we considered only $A\beta$ 1–42 and t-tau measurements.

1.3. FDG-PET

FDG-PET scanning was performed on multiple PET instruments of differing resolutions. FDG-PET scans were collected as 6 5-minute frames from 30 to 60 minutes after injection of approximately 5 mCi of tracer. Scans were corrected with either segmented transmission data or CT scans, depending on instrumentation.

All scans underwent quality control at University of Michigan and were preprocessed to make them more uniform and make PET images from different systems more similar according to the following procedure: raw PET images from all sites were converted to the standard DICOM format; separate frames were coregistered lessening the effects of patient motion, and recombined into a coregistered dynamic image set; coregistered frames were averaged to create a single 30 minute PET image; each resulting image was reoriented into a standard $160 \times 160 \times 96$ voxel image grid having 1.5 mm cubic voxels and oriented such that the anterior-posterior axis of the subject is parallel to the AC-PC line, and intensity normalized using a subject-specific mask with an average voxel intensity of one; each image was finally filtered with a scanner-specific filter function to a common uniform isotropic resolution of 8 mm

FWHM. More detailed information can be found at www.loni.ucla.edu/ADNI/Data/ADNI_Data.shtml.

All pre-processed PET data were analyzed at the University of Utah (Norman Foster laboratory). Pet images were resampled into a Talairach atlas registration using Neurostat stereo v 8.0, and metabolic glucose activity pixel values were extracted and projected onto surface maps using 3D-SSP. Detailed information are available at https://www.loni.ucla.edu/twiki/pub/ADNI/ADNIPostProc/UUtah_Analysis.pdf.

The average cerebral metabolic rate of glucose consumption (CMRglc) in frontal, parietal and temporal cortices normalized to pons was computed and used in the current study as measure of cerebral metabolism.

1.4. Magnetic resonance imaging

ADNI MRI scans were collected at multiple sites using either a GE, Siemens, or Philips 1.5-T system. Two high-resolution T1-weighted volumetric MP-RAGE scans were collected for each subject. Parameter values varied depending on scanning site and can be found at www.loni.ucla.edu/ADNI/Research/Cores/. Each MRI underwent a quality control evaluation at Mayo Clinic. Examinations were evaluated for the presence of structural abnormalities; presence and severity of common artifacts (e.g. blurring due to head motion) were indicated, and one of the two MP-RAGE scans was recommended for use.

MP-RAGE images underwent specific preprocessing correction steps: a system specific correction of image geometry distortion due to gradient nonlinearity, an image intensity nonuniformity correction using the B1 calibration scans, and a further nonuniformity correction using N3 histogram peak sharpening algorithm; the need to perform such preprocessing steps varied with manufacturer and system RF coil configuration. More detailed information can be found at www.loni.ucla.edu/ADNI/Data/ADNI_Data.shtml.

Left and right hippocampal volumes were semiautomatically computed at University of California, San Francisco, using a commercially available high dimensional brain mapping tool (Medtronic Surgical Navigation Technologies (SNT), Louisville, CO) based on fluid image transformation (Christensen et al., 1997) and previously validated (intra-class coefficient > 0.94) (Hsu et al., 2002). The software requires to manually place 2 global landmarks on AC and PC location for data reslice along AC-PC plane, and 44 local landmarks surrounding the left and right hippocampus; once scans are fully landmarked, they are processed by Medtronics algorithms, which produce hippocampal boundaries and volumes; boundaries are checked by qualified reviewers and in case of failure can be manually edited.

In the current study, individual left and right hippocampal volumes were averaged to have a single hippocampal volume measure.

1.5. Statistical analysis

All statistical analyses were carried out using the R statistical software (www.r-project.org/).

Significance of difference among the four groups was assessed by one-way ANOVA for all continue variables, and by the nonparametric χ^2 test for categorical variables, i.e. gender and APOE. Post-hoc Tukey HSD test was used to estimate the between-group differences. For all comparisons, the significance threshold was set at 0.05.

Mean and standard deviation from the group of healthy controls were used to Z-transform all subjects and patients individual biomarker values at baseline ($A\beta$ 1–42, t-tau, FDG metabolism and hippocampal volumes) according to the following formula: $Z\text{-biomarker}^i(\text{subject}^j) = (\text{biomarker}^i(\text{subject}^j) - \text{mean-biomarker}^i(\text{CN}))/\text{SD-biomarker}^i(\text{CN})$, to have standardized measures.

1.6. Biomarker dynamics

To investigate biomarker dynamics, all subjects and patients were ordered based on their Alzheimer's disease assessment scale-cognitive (ADAS-Cog) score (classic 70 point total), which was considered as a surrogate marker of time since AD developed (AD stage). As each biomarker has been shown to change over time, with rates of change following a nonlinear time course, likely sigmoid shaped (Carlson et al., 2008; Chan et al., 2003; Jack et al., 2008b; Jack et al., 2010; Ridha et al., 2006), for each biomarker individual Z scores, after being polarized to have increasing Z scores for increasing disease stage, were plotted against ADAS-Cog scores and the three parameters (asym, xmid and scal) of the generic sigmoid curve ($y = \text{asym}/(1 + \exp((x\text{mid}-x)/\text{scal}))$), Figure 1) were fitted using a nonlinear least square algorithm (nls function of the R software); for each of the fitted parameters, 95% confidence intervals were computed, and R^2 was used as a measure of goodness of fit. The statistical difference between parameters estimated for different biomarkers was assessed looking at the overlap of the 84% confidence intervals, which were shown to give an approximate $\alpha = 0.05$ test (95% intervals giving very conservative results) under the assumption of approximately equal standard errors (Payton et al., 2003).

For each biomarker, the sigmoid fit was compared with the linear fit. Goodness of fits was first assessed comparing sum of squares. In case linear sum of squares was higher than sigmoid one (suggesting sigmoid fit could be better than linear one), an F test was run to compare the relative increase in sum of squares with the relative increase in degree of freedom (linear model having 1 degree of freedom more than sigmoid model): F ratio was computed using the following formula:

$$F = [(\text{linear SS} - \text{sigmoid SS})/(\text{linear d.f.} - \text{sigmoid d.f.})] / \text{sigmoid SS}/\text{sigmoid d.f.}$$

with SS = sum of square, and d.f. = degrees of freedom, and, in case F ratio was higher than 1 (further suggesting

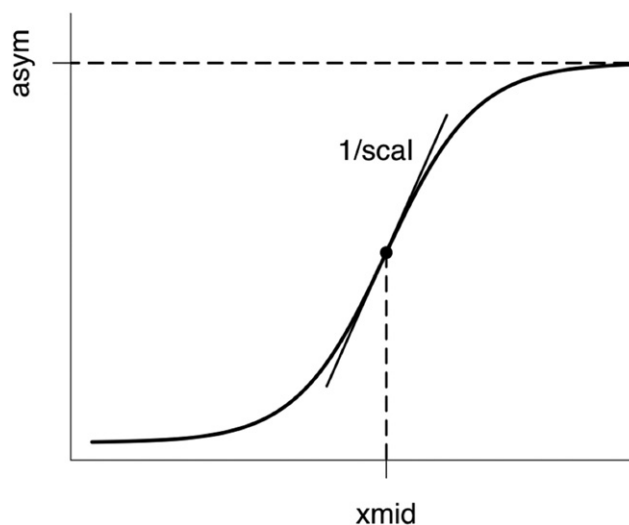


Fig. 1. Schematic representation of the generic sigmoid curve ($y = \text{asym}/(1 + \exp((x\text{mid}-x)/\text{scal}))$). Asym is the asymptote, xmid the inflection point x-value (distance from origin), and one/scal is the angular coefficient of the tangent (i.e. the slope) at point of inflection.

that sigmoid fit could be better), the pertinent p value was computed (F test, numerator d.f. = linear d.f. – sigmoid d.f., denominator d.f. = sigmoid d.f.) to find out whether the sigmoid fit was significantly better than the linear one.

Subjects and patients included in the study were then divided into two groups according to APOE genotype ($\epsilon 4$ carriers and $\epsilon 4$ non carriers), biomarker dynamics was further investigated, and fitted sigmoid curves were computed for each of the two groups.

2. Results

Based on the criteria described in the previous section, 229 healthy controls (age = 76 ± 5 years, 48% females), 154 MCI patients converted to AD (age = 74 ± 7 years, 39% females, conversion time = 17 ± 8 [6–36] months), and 193 AD patients (95 early AD, aged 75 ± 7 years, 45% females, and 98 late AD, aged 75 ± 8 years, 49% females) from ADNI dataset were included in this study.

Table 1 shows main sociodemographic, clinical and neuropsychological features of the four groups of subjects enrolled in the study: the groups did not significantly differ in age and gender but differed in education, healthy subjects and MCI patients having higher education than AD patients; as expected, significant differences in MMSE and ADAS-Cog scores were found, reflecting different stage of cognitive impairment among the groups; APOE $\epsilon 4$ prevalence was found to be significantly different among the groups due to the large difference between cognitively healthy group (27% carriers) and the other three groups (MCI converted to AD: 69%, early AD: 68%, and late AD: 66% carriers), confirming that all patients included in the study, despite being at different stage of the disease, are affected

Table 1
Sociodemographic, clinical and neuropsychological features of ADNI healthy controls, MCI converted to AD, early and late AD patients

	Healthy controls (n = 229)	MCI converted AD (n = 154)	Early AD (n = 95)	Late AD (n = 98)	<i>p</i>
Age, years	76 ± 5	74 ± 7	75 ± 7	75 ± 8	0.52
Gender, females	110 (48%)	60 (39%)	43 (45%)	48 (49%)	0.29
Education, years	16 ± 3	16 ± 3	15 ± 3	14 ± 3	< 0.0001
MMSE	29 ± 1	27 ± 2	25 ± 1	22 ± 2	< 0.0001
ADAS-Cog, classic 70	6 ± 3	13 ± 4	16 ± 5	20 ± 7	< 0.0001
Clock drawing test	4.6 ± 0.7	3.9 ± 1.1	3.7 ± 1.2	3.1 ± 1.3	< 0.0001
AVLT (immediate recall)	43.0 ± 9.8	27.2 ± 6.4	24.1 ± 7.3	21.9 ± 8.2	< 0.0001
Digit span – forward	8.8 ± 2.0	8.3 ± 2.0	7.8 ± 1.7	7.3 ± 2.1	< 0.0001
Digit span – backward	7.2 ± 2.2	6.0 ± 1.8	5.2 ± 1.9	4.6 ± 1.9	< 0.0001
Category fluency (anim.)	19.9 ± 5.6	15.4 ± 4.9	13.3 ± 4.6	11.4 ± 5.0	< 0.0001
Category fluency (veg.)	14.7 ± 3.9	10.0 ± 3.2	8.4 ± 3.3	7.2 ± 3.3	< 0.0001
Trail making test A	36 ± 13	50 ± 26	64 ± 35	70 ± 39	< 0.0001
Trail making test B	89 ± 44	153 ± 82	177 ± 92	198 ± 98	< 0.0001
Digit symbol	45.7 ± 10.2	34.0 ± 11.2	29.0 ± 12.6	23.8 ± 13.5	< 0.0001
Boston naming	27.8 ± 3.0	25.0 ± 4.3	23.6 ± 5.9	20.3 ± 7.6	< 0.0001
AVLT (30 min delayed)	7.4 ± 3.7	1.6 ± 2.4	0.8 ± 1.5	0.7 ± 1.7	< 0.0001
ANART	9.7 ± 9.1	13.6 ± 9.2	14.2 ± 10.0	16.9 ± 10.3	< 0.0001
APOE, carriers	61 (27%)	107 (69%)	65 (68%)	62 (63%)	< 0.0001

p denotes difference significance among all groups on one-way ANOVA (continuous variables) or χ^2 test (categorical variables).

Values are mean ± standard deviations (continuous variables) or frequencies (categorical values, i.e. gender and APOE).

MMSE, Mini Mental State Examination; ADAS-Cog, Alzheimer's disease assessment scale-cognitive; ANART, American national adult reading test; AVLT, auditory verbal learning test–version A; Digit symbol, WAIS-R digit symbol substitution test.

by AD. In all tests of the neuropsychological battery, a significant difference ($p < 0.0001$) among the groups was observed.

About half of the healthy subjects (114/229) and patients (181/347) considered in the current study underwent lumbar puncture thus having CSF $A\beta$ 1–42 and tau data available; half of subjects and patients underwent FDG-PET imaging, and slightly less had data available due to technical failures; all of them underwent MR imaging and more than a half had hippocampal volume available (Table 2).

Tau was significantly different among groups ($p < 0.0001$), healthy controls having the lowest mean value and patients at increasing stage of AD having increasing mean values; Z-scores reflected the monotonous increase. All AD groups were found to be significantly different in CSF tau concentration from healthy controls on post-hoc analysis, while no significant difference was found between AD groups. $A\beta$ 1–42 was significantly different among groups ($p < 0.0001$), and healthy controls $A\beta$ 1–42 mean value was much higher than patient ones; patients at different

Table 2
AD biomarkers in ADNI healthy controls, MCI converted to AD, early and late AD patients

	Healthy controls	MCI converted AD	Early AD	Late AD	<i>p</i>
Tau					
n	114	79	57	45	
pg/mL	69.7 ± 30.4	110.3 ± 51.1	113.9 ± 61.2	125.8 ± 57.6	< 0.0001
Z-score	0.00 ± 1.00	1.41 ± 1.75	1.54 ± 2.09	1.94 ± 1.97	
$A\beta$ 1–42					
n	114	79	57	45	
pg/mL	205.6 ± 55.1	141.9 ± 43.9	144.3 ± 45.8	141.3 ± 33.9	< 0.0001
Z-score	0.00 ± 1.00	1.25 ± 0.82	1.21 ± 0.86	1.27 ± 0.63	
FDG-PET					
n	102	67	53	44	
CRMglc	1.39 ± 0.12	1.29 ± 0.11	1.29 ± 0.10	1.23 ± 0.12	< 0.0001
Z-score	0.00 ± 1.00	0.84 ± 0.94	0.87 ± 0.88	1.35 ± 1.02	
Hippocampal volume					
n	159	119	63	66	
mL	2155 ± 297	1739 ± 363	1654 ± 356	1599 ± 323	< 0.0001
Z-score	0.00 ± 1.00	1.43 ± 1.25	1.73 ± 1.23	1.92 ± 1.11	

p denotes difference significance among all groups on one-way ANOVA.

Values are mean ± standard deviations.

Mean and standard deviation from the subgroup of cognitive normal subjects were used to compute Z scores.

Hippocampal volumes were averaged over left and right.

FDG-PET is the average cerebral metabolic rate of glucose consumption in frontal, parietal and temporal cortices normalized to pons.

disease stage had similar $A\beta$ 1–42 mean values, both in terms of absolute values and Z-score, suggesting that $A\beta$ 1–42 load could be almost disconnected from the disease stage. On post-hoc analysis, all AD groups were found to be significantly different in $A\beta$ 1–42 concentration from healthy controls, while no significant difference was found between AD groups. Mean CRMglc in frontal, parietal and temporal cortices was significantly different among groups ($p < 0.0001$); healthy controls had the highest CRMglc mean values, MCI converted to AD and early AD had comparable values while late AD had the lowest ones (both in terms of absolute values and Z scores), as mean CRMglc mostly decreased in the presymptomatic stage and continued to slightly decrease even at latest stages. On post-hoc analysis, all AD groups were significantly different in CRMglc mean values from healthy controls, MCI converted to AD were significantly different from late AD ($p = 0.04$), and early AD were almost significantly different from late AD ($p = 0.08$), while no difference was found between MCI converted to AD and early AD. Hippocampal volume was significantly different among groups ($p < 0.0001$),

healthy controls having the highest mean value and patients at increasing stage of AD having decreasing mean values; Z-scores reflected the monotonous increase (table 2). All AD groups were significantly different in hippocampal volume from healthy controls on post-hoc analysis, MCI converted to AD were significantly different from late AD ($p = 0.03$), while no difference was found between early AD and either MCI converted to AD or late AD.

Figure 2 shows, for each biomarker, the individual Z scores plotted against ADAS-Cog scores; fitted sigmoid curves are overlapped. Table 3 shows the fitted sigmoid parameters, representing the asymptote (asym), the inflection point x-value (xmid), and the steepness (one/scal) of the sigmoid curve, with 95% confidence intervals. As Z scores are quite dispersed, R^2 coefficients, measuring the goodness of fit, are quite low; the sigmoid curve seems to fit $A\beta$ 1–42 and hippocampal volume ($R^2 = 0.256$ and 0.279 , respectively) better than tau and FDG-PET ($R^2 = 0.137$ and 0.201 , respectively). Comparing the fitted sigmoid curves, the FDG-PET inflection point x-value was found to be significantly different from all the other ones.

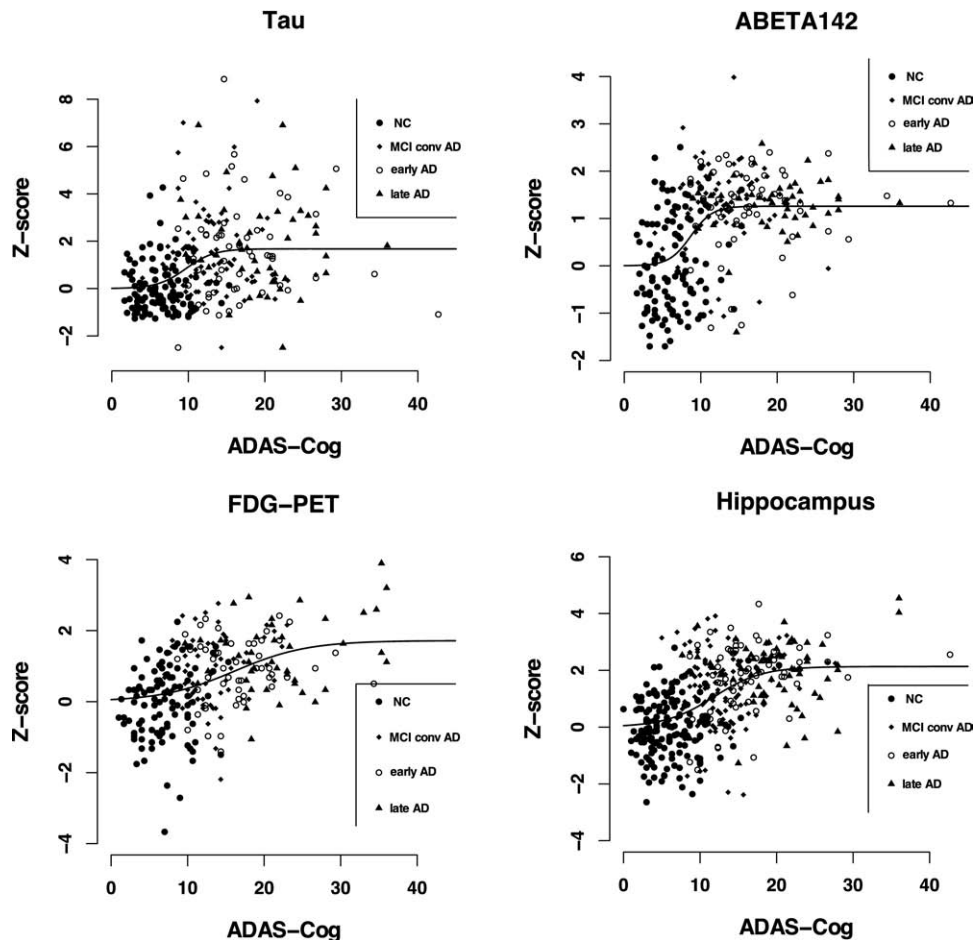
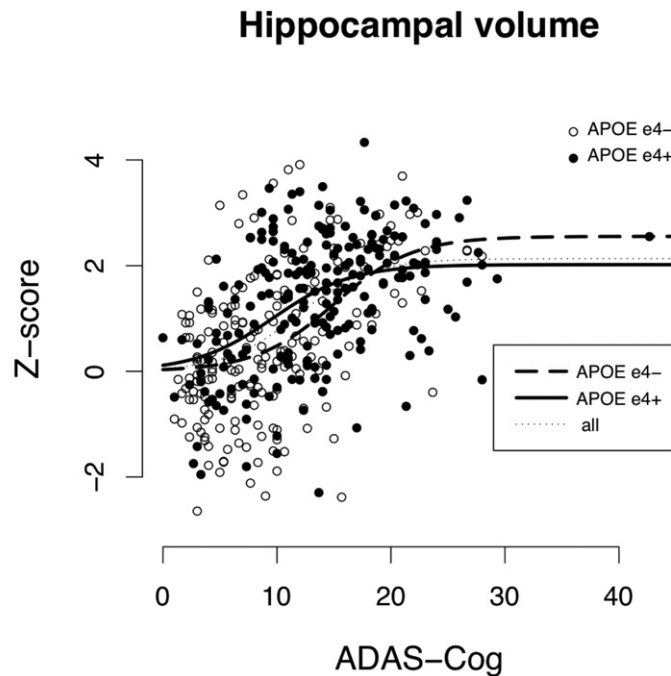


Fig. 2. For each biomarker, individual Z scores are plotted against ADAS-Cog scores, and the fitted sigmoid curve is displayed. Full circles denote healthy controls, full squares MCI patients converted to AD, empty circles early AD, and full triangles late AD patients. Sigmoid fitting was better than linear fitting for Tau, $A\beta$ 1–42 and hippocampus (for the latter: sigmoid nonsignificantly better than linear); linear fitting was better for FDG-PET.



	asym	xmid	scal
All	2.13 [1.76 to 2.51]	11.82 [9.98 to 13.66]	3.18 [1.78 to 4.57]
APOE ε4+	2.02 [1.63 to 2.40]	9.67 [7.40 to 11.94]	3.44 [1.28 to 5.59]
APOE ε4-	2.55 [1.50 to 3.61]	15.02 [10.72 to 19.32]*	3.44 [1.16 to 5.72]

Fig. 3. Individual hippocampal volume Z scores are plotted against ADAS-Cog for both APOE $\epsilon 4$ carriers (full circles), and non-carriers (empty circles). The fitted sigmoid curves for the whole population (thin dotted), APOE $\epsilon 4$ carriers (thick solid), and non-carriers (thick dashed) are displayed.

The parameters of each of the three fitted sigmoids are reported in the bottom table. Values are fitted parameters [95% confidence interval], and * denotes significant difference in APOE $\epsilon 4$ carriers vs non-carriers.

For all biomarkers except FDG-PET, the linear was higher than the sigmoid sum of squares ($A\beta$ 1–42: 268.93 v. 246.21; tau: 860.33 v. 828.09; hippocampal volume: 576.71 v. 573.23) and the sigmoid fit was significantly better than the linear for $A\beta$ 1–42 and tau ($A\beta$ 1–42: $F = 26.94$, $p < 0.0001$; tau: $F = 11.37$, $p < 0.001$, hippocampal volume: $F = 2.45$, n.s.). For FDG-PET, the linear sum of squares was slightly lower than the sigmoid one (255.11 and 260.05, n.s.), suggesting that the linear fit could be better than that of the sigmoid model.

Among the 576 subjects and patients included in the study, 295 were APOE $\epsilon 4$ carriers and 281 non carriers. Of these, 150 $\epsilon 4$ carriers and 145 non carriers had valid CSF $A\beta$ 1–42 and tau values, 218 $\epsilon 4$ carriers and 189 non carriers had valid hippocampal volume values, and 135 $\epsilon 4$ carriers and 131 non carriers had valid FDG-PET data. Fitted sigmoid curves could not be computed for CSF tau and FDG-PET in APOE $\epsilon 4$ carriers, and for $A\beta$ 1–42 in non carriers due to failure of the fit to converge.

The sigmoid fit of hippocampal volume in APOE $\epsilon 4$

Table 3

Fitted sigmoid parameters. Individual Z scores were plotted against ADAS-Cog scores and the three parameters (asym, xmid and scal) of the generic sigmoid curve ($y = \text{asym}/(1 + \exp((\text{xmid}-x)/\text{scal}))$) were fitted using a nonlinear least square algorithm. Sigmoid was better than linear fit for CSF $A\beta$ 1–42, tau and hippocampal volume (for the latter: sigmoid nonsignificantly better than linear); linear fitting was better for FDG-PET.

	asym	xmid	scal	R^2
Tau	1.68 [1.31–2.05]	9.67 [7.72–11.62]	1.85 [0.14–3.56]	0.137
$A\beta$ 1–42	1.26 [1.09–1.43]	8.71 [7.58–9.83]	1.40 [0.41–2.40]	0.256
FDG-PET	1.72 [1.07–2.37]	16.13 [11.16–21.09]*	4.77 [1.88–7.65]	0.201
Hippocampal volume	2.13 [1.76–2.51]	11.82 [9.98–13.66]	3.18 [1.78–4.57]	0.279

Values are fitted parameters [95% confidence interval].

* Denotes significant difference versus all other estimated parameters.

carriers was found to be significantly steeper than the one related to non carriers, and the points of inflection of the two curves on the x-axis were significantly different, indicating that carriers developed hippocampal atrophy earlier in the disease course (Figure 3).

3. Discussion

In the current study we considered a group of healthy controls and three groups of Alzheimer's patients with increasing cognitive impairment, which could be considered as representative of the neurobiological continuum of the disease, and we investigated the dynamics of four of the most validated AD biomarkers: CSF A β 1–42, CSF tau, hippocampal volume and FDG uptake on PET.

Both CSF tau and hippocampal volume showed a monotonous trend, patients with increasingly severe AD showing increasing values of tau and decreasing hippocampal volumes. This is in line with previous evidence that both CSF tau (Arai et al., 1995; Blennow et al., 1995; Buerger et al., 2006; Tapiola et al., 2009) and hippocampal volume (Jack et al., 2000; Schuff et al., 2009) are valid biomarkers of neurodegeneration, and they both correlate with disease severity during the whole time course of the disease (Arai et al., 1995; Hansson et al., 2006; Jack et al., 2000; Schuff et al., 2009; Shaw et al., 2009; Tapiola et al., 2009; Vemuri et al., 2009).

As expected, AD patients at different disease stage showed similar A β 1–42 load (much lower than healthy controls), in agreement with previous evidence that plaque deposition occurs before neurodegeneration and by the time a person has dementia it becomes almost disconnected from the disease duration and severity (Chételat et al., 2010; Ingelsson et al., 2004; Jack et al., 2008a; Jack et al., 2009). As for FDG-PET, preclinical and early AD showed comparable CRMglc mean values, while late AD showed further reduced metabolism. This is in line with previous evidence that alterations in glucose metabolism, reflecting synaptic function and density, already occurs at a preclinical stage (de Leon et al., 2001; Jagust et al., 2006; Mosconi et al., 2009; Reiman et al., 1996; Small et al., 1995), and accompany neurodegeneration, progressive reductions correlating with disease severity (Hoffman et al., 2000; Minoshima et al., 1997; Mosconi et al., 2009).

To our knowledge, this is the first study testing the model of AD biomarker dynamics recently proposed by Jack Jr and colleagues (Jack et al., 2010) on real data. The ongoing ADNI, which has been recently shown to have successfully recruited a large cohort of healthy controls, MCI and AD patients very similar to those seen in MCI and mild AD clinical trials (Petersen et al., 2010), could be considered at present as the gold standard dataset for the study of Alzheimer's disease, and thus the best data choice. In the model, each biomarker was hypothesized to follow a nonlinear and sigmoid-shaped time course. The generic sigmoid function

($y = \text{asym}/(1 + \exp((x_{\text{mid}}-x)/\text{scal}))$), Figure 1) is defined by three parameters: the horizontal asymptote (asym), which gives an indication of the time (disease stage) when the biomarker stabilizes, the x-value at inflection point (x_{mid}), representing the time when maximum variation occurs (most relevant time when to monitor the biomarker to have indications of disease progression), and the steepness of the curve ($1/\text{scal}$), which is a measure of the rate of change.

In this study we showed that different sigmoid curves could actually be used to describe each biomarker time course. Despite individual Z scores being quite dispersed, and thus fitted curves having low R^2 coefficients, fitted sigmoid curves are still meaningful: A β 1–42 fitted sigmoid is steep, has its maximum variation and stabilizes early in time (i.e. in nonpathological ADAS-Cog range), in line with previous evidence of plaque deposition mainly occurring in the preclinical phase (Ingelsson et al., 2004; Jack et al., 2008a; Jack et al., 2009) and with Jack's model (Jack et al., 2010); CSF tau and hippocampal volume fitted sigmoids have similar shapes (in terms of asymptote, rate of change and steepness), in agreement with the notion that they are both markers of neurodegeneration and their change reflects disease progression during the whole time course, and they could be considered late biomarkers (Jack et al., 2010); FDG-PET fitted sigmoid starts to increase early in time, in line with previous evidence of preclinical alterations in glucose metabolism (Jagust et al., 2006; Mosconi et al., 2009), and seems to reach a steady state only at latest stages of the disease, reflecting metabolism reduction occurring during the whole time course of the disease (Jack et al., 2010).

Furthermore, for three of the four biomarkers under study (CSF A β 1–42, tau and hippocampal volume) the sigmoid model was found to fit biomarker dynamics better than the linear model (significantly better for both A β 1–42 and tau). This is an interesting finding, which provides the first evidence to the model proposed by Jack and colleagues (Jack et al., 2010).

It would be now extremely important to compare biomarker dynamics, and order biomarker changes in time to express the disease process in terms of a series of testable biological indicators. However, before fitted curves could be directly compared, some considerations need to be introduced, showing that significant differences reported in Table 3 should be taken with caution. Although each biomarker sigmoid curve was fitted on individual Z-transformed scores to standardize different biomarker values making them comparable, the use of such Z scores has an intrinsic problem. For each biomarker, Z scores were computed based on mean and standard deviations of the healthy controls group, and thus strongly depend on the variability of the biomarker within healthy controls. As variability is due both to measurement error and biological variability, and different biomarkers may have different measurement errors, the variability due to measurement error should ide-

ally be eliminated before computing *z*-scores. Studies assessing and comparing the reliability of each biomarker (i.e. reproducibility studies with repeated measures) are needed to remove the effect of measurement error and compute corrected *Z*-scores that reflect biological variability only. This is likely the reason why, directly comparing FDG-PET versus hippocampal volume fitted curves, FDG-PET seems to have a later rise, in contrast to previous findings (Reiman et al., 1998).

The sigmoid curves describing hippocampal volume change fitted for APOE ϵ 4 carriers and non-carriers were found to be significantly different: the one related to APOE ϵ 4 carriers was significantly steeper than the one related to non carriers, and its point of inflection *x*-values was significantly shifted to the left, suggesting that in APOE ϵ 4 carriers hippocampal atrophy occurs earlier in time.

This finding is in line with a recent study suggesting that APOE ϵ 4 may alter the relationship between biomarkers and cognitive state (Vemuri et al., 2010), and with previous evidence that APOE ϵ 4 carriers have smaller hippocampal volume (Reiman et al., 1998) and faster hippocampal loss (Schuff et al., 2009); this finding further supports the validity of the model proposed by Jack and colleagues (Jack et al., 2010).

To set patients along the disease stage continuum, either a biological or a clinical strategy could be adopted. For the purpose of studying biomarker dynamics no biological variable could be chosen without falling into logical recursivity, and a clinical variable (e.g. ADAS-Cog score) thus needed to be used.

Biomarker differences among groups of AD patients at different disease stages have been interpreted as biomarker changes occurring during the disease course. Current findings, achieved by cross-sectional analysis, should be considered as preliminary, and need to be verified through a truly longitudinal analysis.

It should be noted that biomarker dynamics has not been assessed on the same subject cohort as, for each biomarker, different subgroups of subjects had data available. It was not feasible to include in the study only subjects with all four biomarkers available as the sample size would have notably decreased (just 105 out of 576 subjects included in the current study had all biomarkers available) and the power of the analysis would have thus been severely reduced. As differences in subgroups used to assess biomarker dynamics could have potentially affected the study, current findings need to be verified on a larger sample with all biomarker data available.

In the current study we did not include stable MCI patients: to assess the biomarker dynamics, as homogeneous as possible groups at different time of the Alzheimer's disease course are needed, and the highly heterogeneous stable MCI group, including patients with incipient AD and with different underlying pathologies, patients who will indeed remain stable and who will revert to cognitively normal status, would have biased the study. Additional

analyses on biomarker dynamics assessed including stable MCI (available online at www.centroalzheimer.it/public/Supplemental_analyses_stableMCI.doc) confirmed the main findings of the current study, despite the shape of the biomarker dynamics, likely due just to the biased composition of the additional group, was found to be closer to linear.

In the current study we did not consider PIB-PET, despite being one of the most validated AD biomarkers, for two main reasons: ADNI PIB processed data available at present are fewer than the other biomarkers; furthermore, PIB-PET has been shown to be substantially related to CSF A β 1–42, the two measures of brain A β deposition producing similar results (Jagust et al., 2009).

All patients included in the study had incipient or mild AD, and biomarker dynamics was thus investigated on a relatively narrow disease continuum. It will be interesting to investigate in the future the dynamic changes both rightward (i.e. later in the disease time course), and leftward (i.e. in the presymptomatic phase), ideally following healthy people in time throughout the whole course of the disease and modeling the thresholds where clinical symptoms occur. It will also be interesting to investigate the effect of co-occurring diseases and conditions on biomarker dynamics. Furthermore, as structural loss and synaptic dysfunction do not occur at the same time throughout the brain (Buckner et al., 2005; Frisoni et al., 2009), it will be interesting to investigate the structural and functional variations in disease-specific cerebral regions (e.g. posterior cingulate, medial temporal, lateral temporal and frontal) during the whole disease time course.

In conclusion, in this study we used the ADNI dataset to provide the first evidence in favor of the dynamic biomarker model proposed by Jack and colleagues (Jack et al., 2010), showing that most of the biomarker' dynamics follow a sigmoid trend. A β 1–42 time course was found to follow a steep curve, stabilizing early in the disease course; CSF tau and hippocampal volume changed later in time and showed similar monotonous trends, reflecting disease progression during the whole disease time course. Hippocampal volume loss was found to be steeper and to occur earlier in time in APOE ϵ 4 carriers than in non-carriers, proving additional evidence of validity of the model. Despite providing only partial support for a temporal shift between different types of pathological brain changes in AD, these findings suggest that, as an early marker, A β 1–42 could be used for clinical trials as inclusion criteria, to select patients with preclinical AD, while markers of neural degeneration and dysfunction (e.g. CSF tau, hippocampal volume and FDG-PET) could be used as outcome measures to investigate the drug effect on neurodegeneration.

Disclosure statement

The authors report no actual or potential conflicts of interest.

Acknowledgements

Data collection and sharing for this project was funded by the ADNI (National Institutes of Health, Grant U01 AG024904). ADNI is funded by the National Institute on Aging, the National Institute of Biomedical Imaging and Bioengineering, and through generous contributions from the following: Abbott, AstraZeneca AB, Bayer Schering Pharma AG, Bristol-Myers Squibb, Eisai Global Clinical Development, Elan Corporation, Genentech, GE Healthcare, GlaxoSmithKline, Innogenetics, Johnson and Johnson, Eli Lilly, and Co., Medpace, Inc., Merck and Co., Inc., Novartis AG, Pfizer, Inc, F. Hoffman-La Roche, Schering-Plough, Synarc, Inc., and Wyeth, as well as nonprofit partners the Alzheimer's Association and Alzheimer's Drug Discovery Foundation, with participation from the US Food and Drug Administration. Private sector contributions to ADNI are facilitated by the Foundation for the National Institutes of Health (www.fnih.org). The grantee organization is the Northern California Institute for Research and Education, and the study is coordinated by the Alzheimer's Disease Cooperative Study at the University of California, San Diego. ADNI data are disseminated by the Laboratory for Neuro Imaging at the University of California, Los Angeles. This research was also supported by NIH Grants P30 AG010129, K01 AG030514, and the Dana Foundation.

References

- Arai, H., Terajima, M., Miura, M., Higuchi, S., Muramatsu, T., Machida, N., Seiki, H., Takase, S., Clark, C.M., Lee, V.M., Trojanowski, J.Q., Sasaki, H., 1995. Tau in cerebrospinal fluid: a potential diagnostic marker in Alzheimer's disease. *Ann Neurol* 38, 649–652.
- Blennow, K., Wallin, A., Agren, H., Spenger, C., Siegfried, J., Vanmechelen, E., 1995. Tau protein in cerebrospinal fluid: a biochemical marker for axonal degeneration in Alzheimer disease? *Mol Chem Neuropathol* 26, 231–245.
- Bobinski, M., de Leon, M.J., Wegiel, J., Desanti, S., Convit, A., Saint Louis, L.A., Rusinek, H., Wisniewski, H.M., 2000. The histological validation of post mortem magnetic resonance imaging-determined hippocampal volume in Alzheimer's disease. *Neuroscience* 95, 721–725.
- Buckner, R.L., Snyder, A.Z., Shannon, B.J., laRossa, G., Sachs, R., Fotenos, A.F., Sheline, Y.I., Klunk, W.E., Mathis, C.A., Morris, J.C., Mintun, M.A., 2005. Molecular, structural, and functional characterization of Alzheimer's disease: evidence for a relationship between default activity, amyloid, and memory. *J Neurosci* 25, 7709–7717.
- Buerger, K., Ewers, M., Pirttilä, T., Zinkowski, R., Alafuzoff, I., Teipel, S.J., deBernardis, J., Kerkman, D., McCulloch, C., Soininen, H., Hampel, H., 2006. CSF phosphorylated tau protein correlates with neocortical neurofibrillary pathology in Alzheimer's disease. *Brain* 129, 3035–3041.
- Carlson, N.E., Moore, M.M., Dame, A., Howieson, D., Silbert, L.C., Quinn, J.F., Kaye, J.A., 2008. Trajectories of brain loss in aging and the development of cognitive impairment. *Neurology* 70, 828–833.
- Chan, D., Janssen, J.C., Whitwell, J.L., Watt, H.C., Jenkins, R., Frost, C., Rossor, M.N., Fox, N.C., 2003. Change in rates of cerebral atrophy over time in early-onset Alzheimer's disease: longitudinal MRI study. *Lancet* 362, 1121–1122.
- Chételat, G., Villemagne, V.L., Bourgeat, P., Pike, K.E., Jones, G., Ames, D., Ellis, K.A., Szoek, C., Martins, R.N., O'Keefe, G.J., Salvado, O., 2010. Masters, C.L., Rowe, C.C. Australian Imaging Biomarkers and Lifestyle Research Group. Relationship between atrophy and beta-amyloid deposition in Alzheimer disease. *Ann Neurol* 67, 317–324.
- Christensen, G.E., Joshi, S.C., Miller, M.I., 1997. Volumetric transformation of brain anatomy. *IEEE Trans Med Imaging* 16, 864–877.
- Clark, C.M., Xie, S., Chittams, J., Ewbank, D., Peskind, E., Galasko, D., Morris, J.C., McKeel, D.W., Jr, Farlow, M., Weitlauf, S.L., Quinn, J., Kaye, J., Knopman, D., Arai, H., Doody, R.S., deCarli, C., Leight, S., Lee, V.M., Trojanowski, J.Q., 2003. Cerebrospinal fluid tau and beta-amyloid: how well do these biomarkers reflect autopsy-confirmed dementia diagnoses? *Arch Neurol* 60, 1696–1702.
- Cummings, J.L., Mega, M., Gray, K., Rosenberg-Thompson, S., Carusi, D.A., Gornbein, J., 2005. The Neuropsychiatric Inventory. Elsevier Saunders, Philadelphia.
- de Leon, M.J., Convit, A., Wolf, O.T., Tarshish, C.Y., DeSanti, S., Rusinek, H., Tsui, W., Kandil, E., Scherer, A.J., Roche, A., Imossi, A., Thorn, E., Bobinski, M., Caraos, C., Lesbre, P., Schlyer, D., Poirier, J., Reisberg, B., Fowler, J., 2001. Prediction of cognitive decline in normal elderly subjects with two- [(18)F] fluoro-2-deoxy-D-glucose/positron emission tomography (FDG/PET). *Proc Natl Acad Sci USA* 98, 10966–10971.
- Edison, P., Archer, H.A., Hinz, R., Hammers, A., Pavese, N., Tai, Y.F., Hottot, G., Cutler, D., Fox, N., Kennedy, A., Rossor, M., Brooks, D.J., 2007. Amyloid, hypometabolism, and cognition in Alzheimer disease: an [11C]PIB and [18F] FDG PET study. *Neurology* 68, 501–508.
- Fagan, A.M., Mintun, M.A., Mach, R.H., Lee, S.Y., Dence, C.S., Shah, A.R., laRossa, G.N., Spinner, M.L., Klunk, W.E., Mathis, C.A., deKosky, S.T., Morris, J.C., Holtzman, D.M., 2006. Inverse relation between in vivo amyloid imaging load and cerebrospinal fluid Abeta42 in humans. *Ann Neurol* 59, 512–519.
- Frisoni, G.B., Lorenzi, M., Caroli, A., Kempainen, N., Nägren, K., Rinne, J.O., 2009. In vivo mapping of amyloid toxicity in Alzheimer disease. *Neurology* 72, 1504–1511.
- Frisoni, G.B., Fox, N.C., Jack, C.R., Jr, Scheltens, P., Thompson, P.M., 2010. The clinical use of structural MRI in Alzheimer disease. *Nat Rev Neurol* 6, 67–77.
- Gosche, K.M., Mortimer, J.A., Smith, C.D., Markesbery, W.R., Snowdon, D.A., 2002. Hippocampal volume as an index of Alzheimer neuropathology: findings from the Nun Study. *Neurology* 58, 1476–1482.
- Hempel, H., Burger, K., Teipel, S.J., Bokde, A.L., Zetterberg, H., Blennow, K., 2008. Core candidate neurochemical and imaging biomarkers of Alzheimer's disease. *Alzheimers Dement* 4, 38–48.
- Hansson, O., Zetterberg, H., Buchhave, P., Londos, E., Blennow, K., Minthon, L., 2006. Association between CSF biomarkers and incipient Alzheimer's disease in patients with mild cognitive impairment: a follow-up study. *Lancet Neurol* 5, 228–234.
- Hoffman, J.M., Welsh-Bohmer, K.A., Hanson, M., Crain, B., Hulette, C., Earl, N., Coleman, R.E., 2000. FDG PET imaging in patients with pathologically verified dementia. *J Nucl Med* 41, 1920–1928.
- Hsu, Y.Y., Schuff, N., Du, A.T., Mark, K., Zhu, X., Hardin, D., Weiner, M.W., 2002. Comparison of automated and manual MRI volumetry of hippocampus in normal aging and dementia. *J Magn Reson Imaging* 16, 305–310.
- Ikonomic, M.D., Klunk, W.E., Abrahamson, E.E., Mathis, C.A., Price, J.C., Tsopelas, N.D., Lopresti, B.J., Ziolk, S., Bi, W., Paljug, W.R., Debnath, M.L., Hope, C.E., Isanski, B.A., Hamilton, R.L., deKosky, S.T., 2008. Post-mortem correlates of in vivo PiB-PET amyloid imaging in a typical case of Alzheimer's disease. *Brain* 131, 1630–1645.
- Ingelsson, M., Fukumoto, H., Newell, K.L., Growdon, J.H., Hedley-Whyte, E.T., Frosch, M.P., Albert, M.S., Hyman, B.T., Irizarry, M.C.,

2004. Early Abeta accumulation and progressive synaptic loss, gliosis, and tangle formation in AD brain. *Neurology* 62, 925–931.
- Jack, C.R., Jr, Petersen, R.C., Xu, Y., O'Brien, P.C., Smith, G.E., Ivnik, R.J., Boeve, B.F., Tangalos, E.G., Kokmen, E., 2000. Rates of hippocampal atrophy correlate with change in clinical status in aging and Alzheimer's disease. *Neurology* 55, 484–489.
- Jack, C.R., Jr, Lowe, V.J., Senjem, M.L., Weigand, S.D., Kemp, B.J., Shiung, M.M., Knopman, D.S., Boeve, B.F., Klunk, W.E., Mathis, C.A., Petersen, R.C., 2008a. 11C PiB and structural MRI provide complementary information in imaging of Alzheimer's disease and amnesic mild cognitive impairment. *Brain* 131, 665–680.
- Jack, C.R., Jr, Weigand, S.D., Shiung, M.M., Przybelski, S.A., O'Brien, P.C., Gunter, J.L., Knopman, D.S., Boeve, B.F., Smith, G.E., Petersen, R.C., 2008b. Atrophy rates accelerate in amnesic mild cognitive impairment. *Neurology* 70, 1740–1752.
- Jack, C.R., Jr, Lowe, V.J., Weigand, S.D., Wiste, H.J., Senjem, M.L., Knopman, D.S., Shiung, M.M., Gunter, J.L., Boeve, B.F., Kemp, B.J., Weiner, M., Petersen, R.C., 2009. Alzheimer's Disease Neuroimaging Initiative Serial PIB and MRI in normal, mild cognitive impairment and Alzheimer's disease: implications for sequence of pathological events in Alzheimer's disease. *Brain* 132, 1355–1365.
- Jack, C.R., Jr, Knopman, D.S., Jagust, W.J., Shaw, L.M., Aisen, P.S., Weiner, M.W., Petersen, R.C., Trojanowski, J.Q., 2010. Hypothetical model of dynamic biomarkers of the Alzheimer's pathological cascade. *Lancet Neurol* 9, 119–128.
- Jagust, W.J., Gitcho, A., Sun, F., Kuczynski, B., Mungas, D., Haan, M., 2006. Brain imaging evidence of preclinical Alzheimer's disease in normal aging. *Ann Neurol* 59, 673–681.
- Jagust, W.J., Reed, B., Mungas, D., Ellis, W., Decarli, C., 2007. What does fluorodeoxyglucose PET imaging add to a clinical diagnosis of dementia? *Neurology* 69, 871–877.
- Jagust, W.J., Landau, S.M., Shaw, L.M., Trojanowski, J.Q., Koeppe, R.A., Reiman, E.M., Foster, N.L., Petersen, R.C., Weiner, M.W., Price, J.C., Mathis, C.A., Alzheimer's Disease Neuroimaging Initiative, 2009. Relationships between biomarkers in aging and dementia. *Neurology* 73, 1193–1199.
- Kaplan, E.F., Goodglass, H., Weintraub, S., 1982. The Boston Naming Test, 2nd Ed. Lea and Febiger, Philadelphia.
- Klunk, W.E., Engler, H., Nordberg, A., Wang, Y., Blomqvist, G., Holt, D.P., Bergström, M., Savitcheva, I., Huang, G.F., Estrada, S., Ausén, B., Debnath, M.L., Barletta, J., Price, J.C., Sandell, J., Lopresti, B.J., Wall, A., Koivisto, P., Antoni, G., Mathis, C.A., Långström, B., 2004. Imaging brain amyloid in Alzheimer's disease with Pittsburgh Compound B. *Ann Neurol* 55, 306–319.
- Minoshima, S., Giordani, B., Berent, S., Frey, K.A., Foster, N.L., Kuhl, D.E., 1997. Metabolic reduction in the posterior cingulate cortex in very early Alzheimer's disease. *Ann Neurol* 42, 85–94.
- Mosconi, L., Mistur, R., Switalski, R., Tsui, W., Glodzik, L., Li, Y., Pirraglia, E., Santi, S., Reisberg, B., Wisniewski, T., de Leon, M.J., 2009. FDG-PET changes in brain glucose metabolism from normal cognition to pathologically verified Alzheimer's disease. *Eur J Nucl Med Mol Imaging* 36, 811–822.
- Olsson, A., Vanderstichele, H., Andreasen, N., De Meyer, G., Wallin, A., Holmberg, B., Rosengren, L., Vanmechelen, E., Blennow, K., 2005. Simultaneous measurement of beta-amyloid(1–42), total tau, and phosphorylated tau (Thr181) in cerebrospinal fluid by the xMAP technology. *Clin Chem* 51, 336–345.
- Payton, M.E., Greenstone, M.H., Schenker, N., 2003. Overlapping confidence intervals or standard error intervals: What do they mean in terms of statistical significance? *J Insect Sci* 3, 34.
- Petersen, R.C., Aisen, P.S., Beckett, L.A., Donohue, M.C., Gamst, A.C., Harvey, D.J., Jack, C.R., Jr, Jagust, W.J., Shaw, L.M., Toga, A.W., Trojanowski, J.Q., Weiner, M.W., 2010. Alzheimer's Disease Neuroimaging Initiative (ADNI): clinical characterization. *Neurology* 74, 201–209.
- Reiman, E.M., Caselli, R.J., Yun, L.S., Chen, K., Bandy, D., Minoshima, S., Thibodeau, S.N., Osborne, D., 1996. Preclinical evidence of Alzheimer's disease in persons homozygous for the epsilon 4 allele for apolipoprotein E. *N Engl J Med* 334, 752–758.
- Reiman, E.M., Uecker, A., Caselli, R.J., Lewis, S., Bandy, D., de Leon, M.J., De Santi, S., Convit, A., Osborne, D., Weaver, A., Thibodeau, S.N., 1998. Hippocampal volumes in cognitively normal persons at genetic risk for Alzheimer's disease. *Ann Neurol* 44, 288–291.
- Reitan, R., 1958. Validity of the Trail-Making Test as an indication of organic brain damage. *Percept Mot Skills* 8, 271–276.
- Rey, A., 1964. *l'Examen Clinique en Psychologie*. Presses Universitaires de France, Paris.
- Ridha, B.H., Barnes, J., Bartlett, J.W., Godbolt, A., Pepple, T., Rossor, M.N., Fox, N.C., 2006. Tracking atrophy progression in familial Alzheimer's disease: a serial MRI study. *Lancet Neurol* 5, 828–834.
- Rosen, W.G., Mohs, R.C., Davis, K.L., 1984. A new rating scale for Alzheimer's disease. *Am J Psychiatry* 141, 1356–1364.
- Rowe, C.C., Ng, S., Ackermann, U., Gong, S.J., Pike, K., Savage, G., Cowie, T.F., Dickinson, K.L., Maruff, P., Darby, D., Smith, C., Woodward, M., Merory, J., Tochon-Danguy, H., O'Keefe, G., Klunk, W.E., Mathis, C.A., Price, J.C., Masters, C.L., Villemagne, V.L., 2007. Imaging beta-amyloid burden in aging and dementia. *Neurology* 68, 1718–1725.
- Schoonenboom, N.S., van der Flier, W.M., Blankenstein, M.A., Bouwman, F.H., Van Kamp, G.J., Barkhof, F., Scheltens, P., 2008. CSF and MRI markers independently contribute to the diagnosis of Alzheimer's disease. *Neurobiol Aging* 29, 669–675.
- Schuff, N., Woerner, N., Boreta, L., Kornfield, T., Shaw, L.M., Trojanowski, J.Q., Thompson, P.M., Jack, C.R., Jr, Weiner, M.W., 2009. Alzheimer's Disease Neuroimaging Initiative. MRI Of hippocampal volume loss in early Alzheimer's disease in relation to ApoE genotype and biomarkers. *Brain* 132, 1067–1077.
- Shaw, L.M., Korecka, M., Clark, C.M., Lee, V.M., Trojanowski, J.Q., 2007. Biomarkers of neurodegeneration for diagnosis and monitoring therapeutics. *Nat Rev Drug Discov* 6, 295–303.
- Shaw, L.M., Vanderstichele, H., Knapik-Czajka, M., Clark, C.M., Aisen, P.S., Petersen, R.C., Blennow, K., Soares, H., Simon, A., Lewczuk, P., Dean, R., Siemers, E., Potter, W., Lee, V.M., Trojanowski, J.Q., Alzheimer's Disease Neuroimaging Initiative, 2009. Cerebrospinal fluid biomarker signature in Alzheimer's disease neuroimaging initiative subjects. *Ann Neurol* 65, 403–413.
- Silbert, L.C., Quinn, J.F., Moore, M.M., Corbridge, E., Ball, M.J., Murdoch, G., Sexton, G., Kaye, J.A., 2003. Changes in premorbid brain volume predict Alzheimer's disease pathology. *Neurology* 61, 487–492.
- Small, G.W., Mazziotta, J.C., Collins, M.T., Baxter, L.R., Phelps, M.E., Mandelkern, M.A., Kaplan, A., La Rue, A., Adamson, C.F., Chang, L., Guze, B.H., Corder, E.H., Saunders, A.M., Haines, J.L., Pericak-Vance, M.A., Roses, A.D., 1995. Apolipoprotein E type 4 allele and cerebral glucose metabolism in relatives at risk for familial Alzheimer disease. *JAMA* 273, 942–947.
- Tapiola, T., Alafuzoff, I., Herukka, S.K., Parkkinen, L., Hartikainen, P., Soininen, H., Pirttilä, T., 2009. Cerebrospinal fluid {beta}-amyloid forty-two and tau proteins as biomarkers of Alzheimer-type pathologic changes in the brain. *Arch Neurol* 66, 382–389.
- Van de Pol, L.A., Hensel, A., van der Flier, W.M., Visser, P., Pijnenburg, Y.A., Barkhof, F., Gertz, H.J., Scheltens, P., 2006. Hippocampal atrophy on MRI in frontotemporal lobar degeneration and Alzheimer's disease. *J Neurol Neurosurg Psychiatry* 77, 439–442.
- Vemuri, P., Wiste, H.J., Weigand, S.D., Shaw, L.M., Trojanowski, J.Q., Weiner, M.W., Knopman, D.S., Petersen, R.C., Jack, C.R., Jr, Alzheimer's Disease Neuroimaging Initiative, 2009. MRI and CSF biomarkers in normal, MCI, and AD subjects: diagnostic discrimination and cognitive correlations. *Neurology* 73, 287–293.

- Vemuri, P., Wiste, H.J., Weigand, S.D., Knopman, D.S., Shaw, L.M., Trojanowski, J.Q., Aisen, P.S., Weiner, M., Petersen, R.C., Jack, C.R., Jr, 2010. Alzheimer's Disease Neuroimaging Initiative. Effect of apolipoprotein E on biomarkers of amyloid load and neuronal pathology in Alzheimer disease. *Ann Neurol* 67, 308–316.
- Wechsler, D.A., 1987. Wechsler Adult Intelligence Scale–Revised. Psychological Corporation, New York.
- Zarow, C., Vinters, H.V., Ellis, W.G., Weiner, M.W., Mungas, D., White, L., Chui, H.C., 2005. Correlates of hippocampal neuron number in Alzheimer's disease and ischemic vascular dementia. *Ann Neurol* 57, 896–903.